International Journal of Heat and Technology
Vol. 38, No. 4, December, 2020, pp. 960-966
Journal homepage: http://iieta.org/journals/ijht

Investigation on the Performance of a Solar Hybrid Refrigeration System Using Environmentally Friendly Fluids

Latra Boumaraf*, Rachedi Khadraoui

LR3MI, Department of Mechanical Engineering, Badji Mokhtar University BP 12, Annaba 23000, Algeria

Corresponding Author Email: boumaraf.latra@univ-annaba.dz

https://doi.org/10.18280/ijht.380423

Received: 20 October 2019
Accepted: 5 September 2020

Keywords:
hybrid refrigeration cycle, ejector, solar energy, environmentally friendly fluids, modeling

ABSTRACT

In order to evaluate the performance of a hybrid compression / ejection refrigeration system using solar energy at low or medium temperature, a simulation model of its behavior based on those of its various components has been developed. It includes in particular for the ejector, a 1-D model of the "constant section mixing" type developed in optimal transition regime. The refrigerants tested are steam for the ejector loop and the R1234yf (replacing the R134a) for the mechanical compression loop. The behavior of the H_2O vapor flowing in the ejector is considered that of the perfect gas. The properties of refrigerants are calculated using REFPROP® software, everywhere else. For a cooling capacity of 10 kW and air conditioning operating conditions, the model allows to determine the main parameters of the ejector and its entrainment ratio, the thermal and mechanical *COP* of the whole refrigeration system as well as the necessary surface of the solar collector. Furthermore, the influence of the temperature of the boiler, the condenser, the intercooler as well as that of the evaporator on the mechanical *COP* of the hybrid system and the solar collection surface in particular, were examined. The results highlight that the solar refrigeration system with hybrid cycle compression/ejection using the refrigerants H_2O/R1234yf allows an increase of the mechanical *COP* higher than 50% compared to that of the conventional refrigeration system and thus constitutes an acceptable ecologically system that can compete with the latter.

1. INTRODUCTION

In the context of sustainable development, the use of an ejector refrigeration system [1] for the production of cold (refrigeration and air conditioning) combines two advantages, one related to the energy saving due to the use of a free energy source (solar energy or heat discharges from industrial processes) and the other related to the protection of the environment through the reduction of CO_2 emissions in the atmosphere. In addition, this type of system is more suitable for the use of refrigerants more environmentally friendly (natural or synthetic with low environmental impact). However, its coefficient of performance, *COP* is closely related to the performance of the ejector determined by its entrainment rate, *U* which is often mediocre. Several studies [2-8] have focused on improving the latter, which is a function of the operating conditions of the system, the geometric parameters of the ejector and the nature of the working fluid. For this purpose, the use of a hybrid refrigeration system compression/ejection overcomes this disadvantage [9]. Indeed, the latter allows combining the advantages and eliminating the disadvantages of both ejector and vapor compression sub-systems. In order to evaluate and optimize the performance of this system, a simulation model of its thermodynamic cycle has been developed. It includes, for the ejector, a 1-D model based on the equations of mass conservation, balance momentum and energy conservation, of "constant section mixing" type in transition mode, developed previously [10-12]. H_2O is used as a refrigerant in the ejector sub-cycle and the R1234yf (*ODP* = 0 and *GWP* = 4) replacing the R134a (*ODP* = 0 and *GWP* = 1430) is used in the mechanical vapor compression sub-cycle. The reference operating temperatures of the generator (boiler), the condenser, the intercooler and the evaporator are respectively set at T_B = 80°C, T_C = 40°C, T_{int} = 30°C and T_E = 5°C. The cooling capacity selected is 10 kW. The entrainment ratio *U* and the main geometrical parameters of the ejector as well as the thermal performance coefficient, COP_{th} and the mechanical performance coefficient, COP_{mec} of the ejection/compression hybrid cycle refrigeration system are then calculated. Furthermore, the influence of the temperature of the boiler, the condenser, the intercooler as well as that of the evaporator on the mechanical *COP* of the hybrid system and the solar collector surface in particular, were examined.

2. SOLAR REFRIGERATION SYSTEM WITH HYBRID EJECTION/COMPRESSION CYCLE

The cycle of a hybrid ejection/compression refrigeration system (Figure 1) consists of a sub-cycle of an ejector refrigeration system (Figure 2(a)) connected to that of a vapor compression system (Figure 2(b)). Steam is used as a refrigerant in the first sub-cycle while R1234yf is used in the second one. The connection between the two sub-cycles is ensured by the intercooler which serves as an evaporator for the ejector sub-cycle and a condenser for the vapor compression sub-cycle. Its operating temperature T_{int} is between the temperature of the evaporator T_E and that of the condenser T_C of the hybrid cycle.

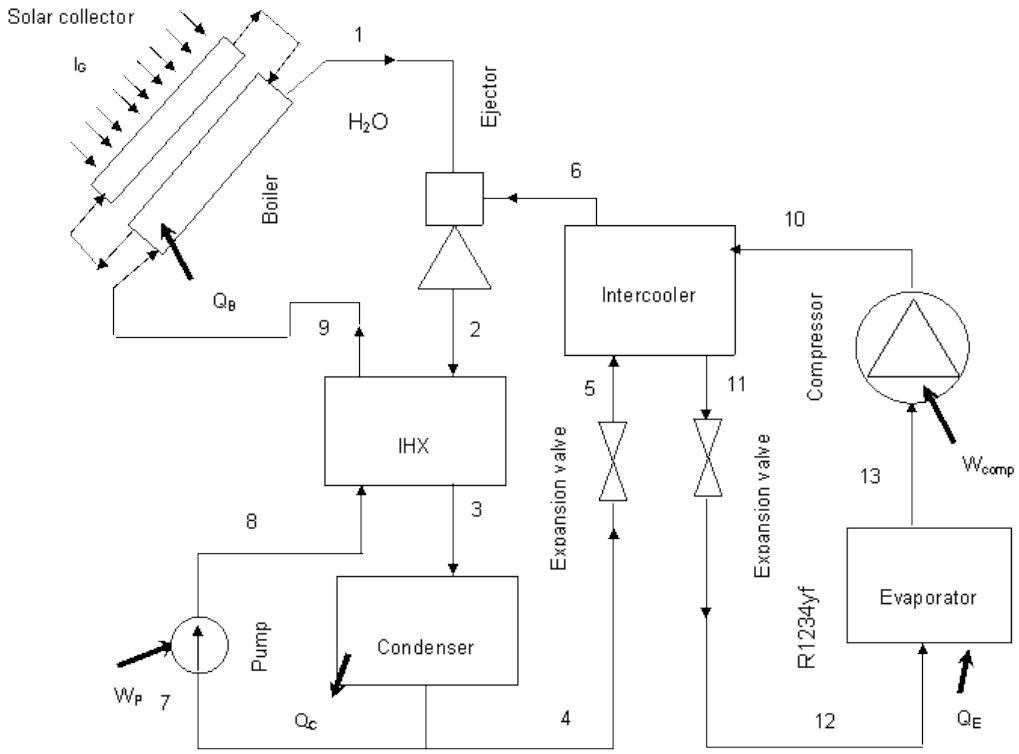

Figure 1. Diagram of the hybrid ejection/compression refrigeration system

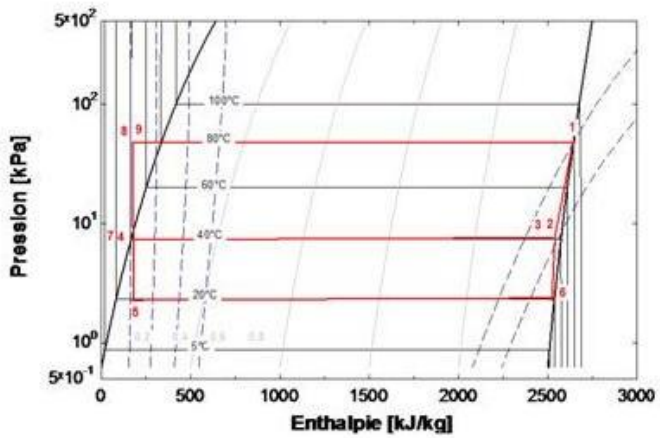

(a)

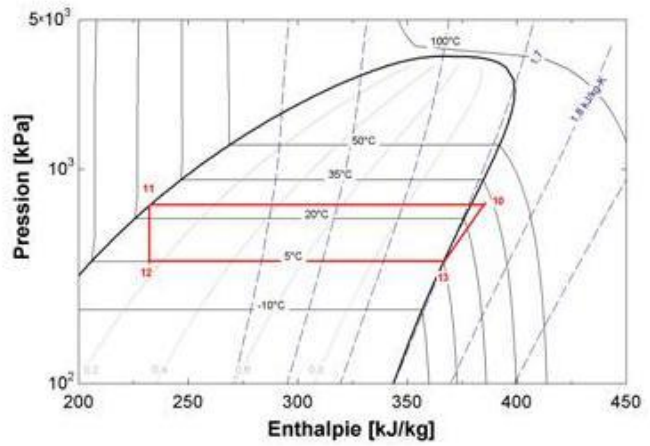

(b)

Figure 2. Diagrams of the ejector (a) and vapor compression (b) sub-cycles of the hybrid ejection/compression refrigeration system

Figure 3 depicts the configuration of the ejector used. An ejector is a static system composed by a primary nozzle whose throat and outlet diameters are respectively d^*_P and d_P. This so-called motive nozzle is disposed in a secondary nozzle, which includes a suction chamber, a mixing chamber (tube cylindrical with diameter d_m) and a diffuser with an outlet diameter of d_D.

The operating cycle of the hybrid ejection/compression refrigeration system is as follows: the supply of thermal energy, Q_B to the boiler from a solar collector, is used to produce H_2O vapor at high temperature and high pressure (state 1) called primary or motive fluid (P) which expands in the ejector primary nozzle (Figure 3). At the outlet, the high-speed primary fluid drives the vapor H_2O called secondary fluid (S) from the intercooler in state 6. Then, the primary and secondary flows mix in the mixing chamber. A first pressure increase due to the formation of a Normal Shock Wave (NSW) takes place in the mixing chamber followed by a second due to compression in the diffuser. At the outlet of the latter, the mixture of superheated steam (state 2) passes into a heat exchanger where its temperature is reduced to that of state 3, before entering the condenser where it passes in liquid form. The condensation heat, Q_C is rejected to the surrounding environment. A part of the condensate, state 4, passes through an expansion device to the state 5 and then enters the intercooler where it is evaporated by the condensation heat of the vapor compression refrigeration sub-cycle operating with the fluid R1234yf. The remainder of condensate H_2O, state 7, is pumped by a circulation pump, state 8 to the boiler, state 9, via the heat exchanger, IHX where it recovers the sensible heat of the H_2O vapor from the ejector. In the vapor compression sub-cycle, the R1234yf vapor from the compressor, state 10, is condensed at the liquid form, state 11, in the intercooler. The heat of this condensation is used to vaporize the refrigerant from the ejector sub-cycle. The condensate, state 11, first undergoes a pressure reduction to that of the state 12 at the passage of an expansion device before entering the evaporator to produce the expected cooling effect Q_E. At the exit of the

latter, R1234yf in the state 13 is compressed by the compressor to the state 10 before entering the intercooler, which completes the hybrid ejection/compression cycle.

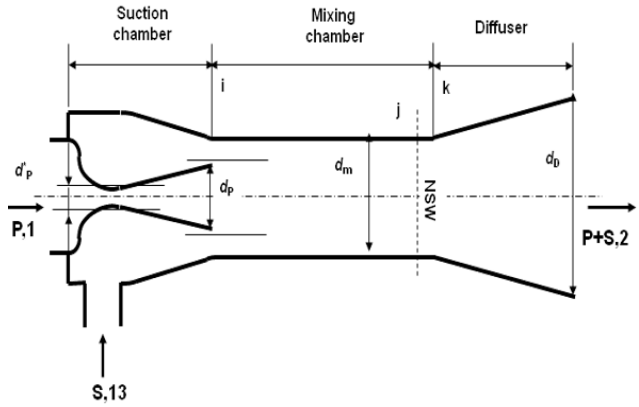

Figure 3. Configuration of the ejector

3. MODELING

3.1 Assumptions

The purpose of the modeling is to determine the thermodynamic characteristics of the fluids (steam and R1234yf) at the various points of the ejector and vapor compression sub-cycles. For this, the following assumptions are made:

- The steams at the outlet of the generator, the intercooler and the evaporator as well as the liquids at the outlet of the condenser and the intercooler are saturated.
- The throttling processes in the expansion valves are considered to be isenthalpic.
- The compressor has a given isentropic efficiency (η_{comp} = 0.75).
- The heat exchanger has a thermal efficiency of 80% and the pump has a mechanical efficiency of 50%.

Moreover, to determine the state of the refrigerant at the inlet of the condenser, it is necessary to model the ejector operation. The assumptions adopted for the study of the ejector are essentially:

- The steam flow in the ejector is considered as that of the perfect gas, everywhere else, the properties of the refrigerants are calculated using the software REFPROP® [13].
- The velocities of the primary fluid at the inlet of the ejector and the mixture at the outlet of the diffuser are assumed to be equal to an arbitrary value of 1 m/s (this allows a complete sizing of the ejector); that of the secondary fluid at the entrance of the ejector is neglected.
- The motive fluid reaches sonic velocity at the primary nozzle throat section.
- The pressure on the plane (i) is assumed to be uniform and equal to that corresponding to the secondary flow choking at the beginning of the mixing process (transition mode).
- The normal shock wave takes place in the cylindrical tube of the secondary nozzle.
- The primary nozzle, the suction chamber of the secondary nozzle and the diffuser have given isentropic efficiencies (respectively η_P = 0.95, η_S = 0.95 and η_D = 0.8) and the friction losses in the mixing chamber are neglected.

3.2 Ejector model

The mathematical equations of the ejector model are obtained by applying the principles of conservation of mass, energy as well as the balance of momentum at judiciously chosen control volumes.

The speed of the primary fluid (P) at the outlet of the convergent-divergent (plane i) is given by:

$$V_{Pi} = \sqrt{2\eta_P \left(h_{P1} - h_{Pi}\right)_{is} + {V_{P1}}^2} \tag{1}$$

The area of the motive flow at the primary nozzle throat, A_P^* and that before mixing (plane i of the ejector), A_{Pi} are computed by:

$$A_P^* = \frac{\dot{m}_P}{\rho_P^* \sqrt{2\eta_P \left(h_{P1} - h_P^*\right)_{is}}} \tag{2}$$

$$A_{Pi} = \frac{\dot{m}_P}{\rho_{Pi} \sqrt{2\eta_P \left(h_{P1} - h_{Pi}\right)_{is}}} \tag{3}$$

The speed of the secondary fluid (S) at the mixing chamber inlet (plane i) is given by:

$$V_{Si} = \sqrt{2\eta_S \left(h_{S6} - h_{Si}\right)_{is}} \tag{4}$$

The area of the secondary flow before mixing (plane i of the ejector) is given by:

$$A_{Si} = \frac{\dot{m}_S}{\rho_{Si} \sqrt{2\eta_S \left(h_{S6} - h_{Si}\right)_{is}}} \tag{5}$$

The speed of the mixture V_j is determined from the balance of the momentum between the planes i and j:

$$V_j = \frac{V_{Pi} + UV_{Si}}{\left(1+U\right)} + \frac{P_{Pi}A_{Pi} + P_{Si}A_{Si} - P_jA_i}{\left(1+U\right)\dot{m}_P} \tag{6}$$

With: $A_i = A_{Pi} + A_{Si}$.

The enthalpy h_j (or temperature T_j) of the mixture is according to the principle of energy conservation:

$$h_j = \frac{h_{Pi} + 1/2{V_{Pi}}^2 + U\left(h_{Si} + 1/2{V_{Si}}^2\right) - 1/2{V_j}^2}{\left(1+U\right)} \tag{7}$$

The corresponding Mach number M_j is then:

$$M_j = \frac{V_j}{\sqrt{\gamma RT_j}} \tag{8}$$

The Mach number of the fluid after passage of the shock wave M_k and the compression ratio P_k / P_j are:

$$M_k = \sqrt{\frac{1 + \left((\gamma-1)/2\right){M_j}^2}{\gamma {M_j}^2 - \left((\gamma-1)/2\right)}} \tag{9}$$

$$\frac{P_k}{P_j} = 1 + \frac{2\gamma}{\gamma+1}\left(M_j{}^2 - 1\right) \tag{10}$$

The enthalpy h_2 and the pressure P_2 of the mixture at the outlet of the diffuser are determined from the following equations:

$$h_2 = \frac{h_{P1} + 1/2 V_{P1}{}^2 + U h_{S6} - 1/2 V_2{}^2}{(1+U)} \tag{11}$$

$$\eta_D = \frac{(h_{2,is} - h_k)}{(h_2 - h_k)} \tag{12}$$

$$P_2 = f(s_{2,is}, h_{2,is}) \tag{13}$$

3.3 Vapor compression sub-cycle model

The cooling capacity $\dot{Q}_E$ is fixed; the mass flow rate of R1234yf circulating in the evaporator $\dot{m}_E$ is given by:

$$\dot{m}_E = \frac{\dot{Q}_E}{(h_{13} - h_{12})} \tag{14}$$

The enthalpy of the refrigerant at the compressor outlet h_{10} is determined from the following equations:

$$\eta_{comp} = \frac{(h_{10,is} - h_{13})}{(h_{10} - h_{13})} \tag{15}$$

With: $h_{10,is}=f(P_{10}, s_{13})$.
Consequently, the compressor consumption power is:

$$\dot{W}_{comp} = \dot{m}_E (h_{10} - h_{13}) \tag{16}$$

The secondary mass flow rate of the ejector $\dot{m}_S$ is calculated from the energy balance of the intercooler:

$$\dot{m}_S = \frac{\dot{m}_E (h_{10} - h_{11})}{(h_6 - h_5)} \tag{17}$$

3.4 Ejector sub-cycle model

The enthalpy of liquid water at the pump outlet (point 8) is determined by:

$$h_8 = h_7 + \frac{(P_8 - P_7)}{\rho_7} \tag{18}$$

Then, the pump consumption power is:

$$\dot{W}_P = \frac{\dot{m}_P (h_8 - h_7)}{\eta_P} \tag{19}$$

The steam temperature T_3 at the outlet of the heat exchanger is calculated from the efficiency ε of the latter:

$$\varepsilon = \frac{T_2 - T_3}{T_2 - T_8} \tag{20}$$

The enthalpy of liquid water at the boiler inlet (point 9) is calculated from the energy balance of the IHX:

$$h_9 = h_8 + (1+U)(h_3 - h_2) \tag{21}$$

With: $h_3=f(P_3=P_C, T_3)$.

3.5 Performance of the hybrid ejection/compression refrigeration cycle

The performance of the hybrid refrigeration system is evaluated using the thermal performance coefficient (COP_{th}) and the mechanical one (COP_{mec}) defined respectively by Eqns. (22) and (24):

$$COP_{th} = \frac{\dot{Q}_E}{\dot{Q}_B + \dot{W}_P + \dot{W}_{comp}} \tag{22}$$

where, $\dot{Q}_B$ is the thermal power of the boiler given by:

$$\dot{Q}_B = \dot{m}_P (h_1 - h_9) \tag{23}$$

$$COP_{mec} = \frac{\dot{Q}_E}{\dot{W}_P + \dot{W}_{comp}} \tag{24}$$

Furthermore, the area of the solar collector A_{SC} can be determined by:

$$A_{SC} = \frac{\dot{Q}_B}{I_G \eta_{SC}} \tag{25}$$

where, I_G is the global incident radiation assumed to be constant and equal to 900 W/m^2 and η_{SC} the efficiency of the solar collector estimated at 50% [14].

4. CALCULATION PROCEDURE

Steam superheating at the outlet of the boiler (point 1), the intercooler (point 6) and the evaporator (point 13) as well as the liquid subcooling at the outlet of the condenser (points 4 and 7) and the intercooler (point 11) are assumed to be zero; the thermodynamic properties at these points are determined using the phase change temperatures of the boiler T_B, the condenser T_C, the intercooler T_{int} and the evaporator T_E. In addition, the refrigeration capacity $\dot{Q}_E$ being fixed, the application of the vapor compression, sub-cycle model allows to calculate the power consumption of the compressor (Eq. (16)), the secondary mass flow rate $\dot{m}_S$ (Eq. (17)) which is an input data for the ejector model. The use of the latter leads to the determination of the main geometric parameters of the ejector, its entrainment ratio U (or primary mass flow rate $\dot{m}_P$) and the thermodynamic properties of the steam at the outlet of the diffuser (state 2). The ejector sub-cycle model uses the output parameters of the previous model to calculate the consumption power of the pump (Eq. (19)) as well as the

thermal power of the boiler (Eq. (23)). Finally, the Eqns. (22), (24) and (25) allow determining respectively the COP_{th}, the COP_{mec} and the surface of the solar collector A_{SC}.

5. RESULTS AND DISCUSSION

On Figure 4, the variations of the entrainment ratio of the ejector U, the COP_{th} and the COP_{mec} of the hybrid refrigeration system are represented as a function of the condenser temperature T_C. It can be seen that the values of U and COP_{th} are higher than those usually encountered in a basic ejector refrigeration system operating in the same conditions. This can be explained by the increase in the pressure of the secondary fluid at the inlet of the ejector into the hybrid refrigeration system. Furthermore, on the same figure, the COP_{mec} of the hybrid system is compared to the COP_{mec} of the conventional vapor compression refrigeration system operating at the same temperatures of the condenser and the evaporator. These results clearly show that in a "useful" temperature range of the condenser, the COP_{mec} of the hybrid system is higher than the COP_{mec} of the conventional vapor compression system. Indeed, for a condenser temperature varying between 35 and 50°C, the increase in COP_{mec} varies from 61 to 42%.

This electrical energy saving achieved in the hybrid system is in fact provided in thermal form by the solar collector.

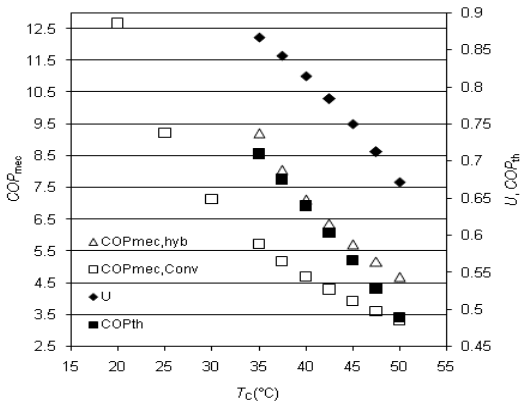

Figure 4. Variations of U, COP_{th}, COP_{mec} of the hybrid refrigeration system and COP_{mec} of the conventional system as a function of T_C for T_B = 80°C, T_{int} = T_C-10 and T_E = 5°C

Figure 5 highlights the fact that the more the mechanical performance of the hybrid system degrades (COP_{mec} decreases) with the increase of the condenser temperature the more the surface of the solar collector increases to produce the same imposed cooling capacity (10 kW).

Logically, Figure 6 shows that the level of the boiler temperature, T_B has no influence on the COP_{mec} of the hybrid system and that the surface of the solar collector, A_{SC} increases when T_B decreases.

At T_B, T_C and T_E fixed Figure 7 shows that U and the COP_{th} increase with the temperature of the intercooler T_{int} while the COP_{mec} decreases with the latter. This can be explained by the fact that the intercooler acts as an evaporator for the ejector loop and as a condenser for the vapor compression loop. This figure also shows that the curves representing the variations of COP_{th} and COP_{mec} as a function of T_{int} intersect at a point whose value of T_{int} is equal to approximately T_C-10 leading to the optimal performance of the hybrid ejection /compression refrigeration system.

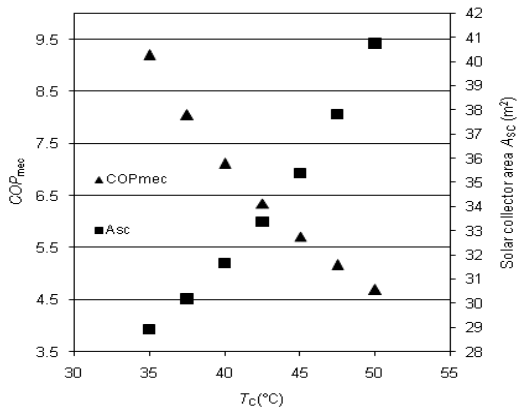

Figure 5. Variations of the COP_{mec} of the hybrid refrigeration system and the solar collector surface A_{SC} as a function of T_C for T_B = 80°C, T_{int} = T_C-10 and T_E = 5°C

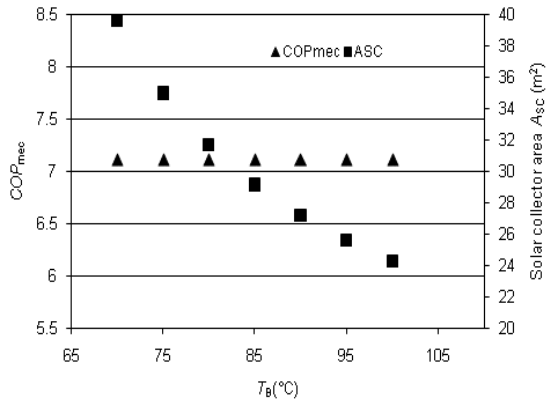

Figure 6. Variations of COP_{mec} of the hybrid refrigeration system and the solar collector surface A_{SC} as a function of T_B for T_C = 40°C, T_{int} = 30°C and T_E = 5°C

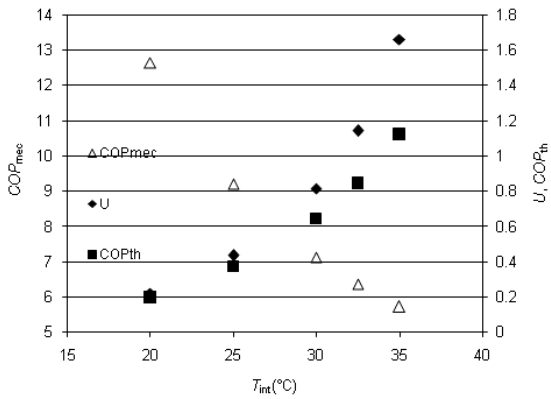

Figure 7. Variations of U, COP_{th} and COP_{mec} of the hybrid refrigeration system as a function of T_{int} for T_B = 80°C, T_C = 40°C and T_E = 5°C

Furthermore, Figure 8 highlights the fact that when the temperature of the intercooler increases, the COP_{mec} of the hybrid system degrades while the surface of the solar collector decreases. This decrease can be explained by a lower contribution of the ejector subsystem in the production of the same cooling capacity.

Figure 9 shows that the variation of the temperature T_E affects not only the vapor compression sub-cycle but also the ejector sub-cycle. Indeed, it shows that when T_E, increases, the COP_{mec} of the hybrid system increases while the surface area of the solar collector A_{SC} decreases.

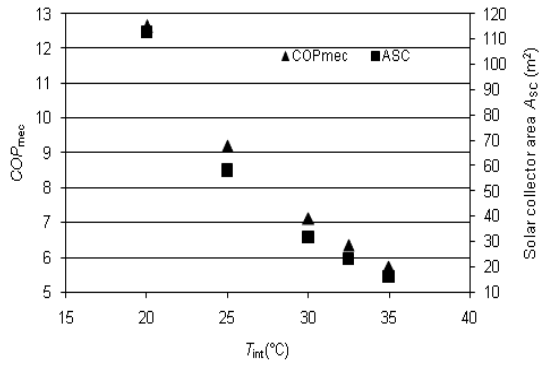

Figure 8. Variations of the COP_{mec} of the hybrid refrigeration system and the solar collector surface A_{SC} as a function of T_{int} for T_B = 80°C, T_C = 40°C and T_E = 5°C

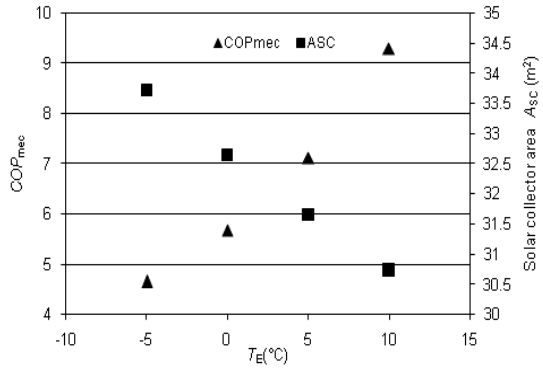

Figure 9. Variations of the COP_{mec} of the hybrid refrigeration system and the solar collector surface A_{SC} as a function of T_E for T_B = 80°C, T_C = 40°C and T_{int} = 30°C

6. CONCLUSIONS

For a cooling capacity and temperatures of the phase change at the boiler, condenser, intercooler and evaporator fixed, the model presented in this work allows to determine the main geometrical parameters of the ejector and its entrainment ratio, the thermal and mechanical coefficient of performance as well as the surface of the solar collector of a hybrid compression / ejection refrigeration system.

In particular, for air conditioning operating conditions, the results obtained show that the hybrid refrigeration system allows to reach COP_{mec} values much better than those of the conventional vapor compression cycle. Indeed, an increase greater than 50% has been observed. This saving in electrical energy, in addition to the use of natural refrigerant (H_2O) and low ecological impact fluid (R1234yf) make the hybrid refrigeration system using solar energy an environmentally acceptable system that can compete with the conventional vapor compression refrigeration system.

This work can be continued by testing other natural fluids such as propane R290 or isobutane R600a.

REFERENCES

[1] Eames, I.W., Aphornratana, S., Haider, H. (1995). A theoretical and experimental study of a small-scale steam jet refrigerator. International Journal of Refrigeration, 18(6): 378-386. http://doi.org/10.1016/0140-7007(95)98160-M

[2] Huang, B.J., Chang, J.M., Wang, C.P., Patrenko, V.A. (1999). A 1-D analysis of ejector performance. International Journal of Refrigeration, 22(5): 354-364. http://doi.org/10.1016/S0140-7007(99)00004-3

[3] Riffat, S.B., Omer, S.A. (2001). CFD modeling and experimental investigation of an ejector refrigeration system using methanol as the working fluid. International Journal of Energy Research, 25(2): 115-128. http://doi.org/10.1002/er.666

[4] Sriveerakul, T., Aphornratana, S., Chunnanond, K. (2007). Performance prediction of steam ejector using computational fluid dynamics: Part 1. Validation of the CFD results. International Journal of Thermal Sciences, 46(8): 812-822. http://doi.org/10.1016/j.ijthermalsci.2006.10.014

[5] Sriveerakul, T., Aphornratana, S., Chunnanond, K. (2007). Performance prediction of steam ejector using computational fluid dynamics: Part 2. Flow structure of a steam ejector influenced by operating pressures and geometries. International Journal of Thermal Sciences, 46(8): 823-833. http://doi.org/10.1016/j.ijthermalsci.2006.10.012

[6] Chunnanond, K., Aphornratana, S. (2004). Ejectors: Applications in refrigeration technology. Renewable and Sustainable Energy Reviews, 8(2): 129-155. http://doi.org/10.1016/j.rser.2003.10.001

[7] Boumaraf, L., Lallemand, A. (1999). Performance analysis of a jet cooling system using refrigerant mixtures. International Journal of Refrigeration, 22(7): 580-589. http://doi.org/10.1016/S0140-07(99)00016-X

[8] Boumaraf, L., Haberschill, P. (2017). performance of a solar-driven ejector refrigerating system using fluids with low ecological impact. International Journal of Energy, Environment and Economics, 24(4): 393-401.

[9] Rusly, E., Aye, Lu, Charters, W.W.S., Ooi, A. (2005). CFD analysis of ejector in a combined ejector cooling system. International Journal of Refrigeration, 28(7): 1092-1101. http://doi.org/10.1016/j.ijrefrig.2005.02.005

[10] Boumaraf, L., Lallemand, A. (2009). Modeling of an ejector refrigerating system operating in dimensioning and off- dimensioning conditions with the working fluids R142b and R600a. Applied Thermal Engineering, 29(2-3): 265-274. http://doi.org/10.1016/j.applthermaleng.2008.02.020

[11] Boumaraf, L., Lallemand, A. (2007). Comparaison des performances optimales d'un éjecteur dimensionné selon les modèles à pression constante et à section constante. In: Proceedings of the 13th International Thermal Meetings, Albi-France, 1: 371-375.

[12] Boumaraf, L., Haberschill, P., Lallemand, A. (2014). Investigation of a novel ejector expansion refrigeration system using the working fluid R134a and its potential substitute R1234yf. International Journal of Refrigeration, 45: 148-159. http://doi.org/10.1016/j.ijrefrig.2014.05.021

[13] NIST Standard Reference Database 23, Version 7.0

[14] Huang, B.J., Petrenko, V.A., Samofatov, I.Y., Shchetinina, N.A. (2001). Collector selection for solar ejector cooling system. Solar Energy, 71(4): 269-274. http://doi.org/10.1016/S0038-092X(01)00042-1

NOMENCLATURE

A	ejector section area, m²
A_{SC}	solar collector surface, m²
COP	coefficient of performance
C_P	constant pressure specific heat, J. kg^{-1}. K^{-1}
d	diameter, m
GWP	Global Warming Potential
h	specific enthalpy, J. kg^{-1}
I_G	global incident solar radiation, W/m^2
M	Mach number
$\dot{m}$	mass flow rate, kg. s^{-1}
ODP	Ozone Depletion Potential
P	pressure, Pa
NSW	Normal Shock Wave (Fig.3)
s	specific entropy, J. kg^{-1}. K^{-1}
Q	heat amount, J
$\dot{Q}$	thermal power, W
R	specific gas constant, J. kg^{-1}. K^{-1}
T	temperature, K or °C
U	ejector entrainment ratio, $\left(=\dot{m}_S/\dot{m}_P\right)$
V	fluid speed, m. s^{-1}
$\dot{W}$	mechanical power, W
w	Specific work, J. kg^{-1}

Greek symbols

ε	heat exchanger efficiency
η	isentropic efficiency
η_{SC}	thermal efficiency of the solar collector
η_P	pump efficiency
ρ	density, kg. m^{-3}

Subscripts, Superscripts

B	boiler
C	condenser
comp	compressor
D	diffuser
E	evaporator
G	global
int	intercooler
is	isentropic process
m	mixing
mec	mechanical
P	primary fluid (or nozzle)
S	secondary fluid (or nozzle)
th	thermal
*	throat section of the primary nozzle
i, j, k	locations in the ejector
1,2,.., 13	locations in the hybrid cycle